Supplementary Figure 1. Limited detection of florescence signals in the intact tumor spheroids by confocal imaging. Optical section images of tumor spheroids stained for type I collagen in PANC-1 spheroids (A) and Ki-67 in HT-29 spheroids (B) with or without tissue clearing process (CLARITY). Signals of type I collagen (A) and Ki-67 (B) were absent in the central region of the spheroids without tissue clearing, indicating limited penetration of antibodies in the immunofluorescence staining. Nuclear DAPI signal was not detected in the central region of PANC-1 spheroids (A), but detected in HT-29 spheroids following refractive index matching (B). Spheroids were cultured either in mini-pillar array (PANC-1) for 7 days or in ULA 96-well plates (HT-29) for 6 days and subjected to immunofluorescence staining with or without tissue clearing procedure and subsequent confocal imaging. Images were obtained by optical sectioning at 20 μm increments from the surface to the core of spheroids along the z-axis. Scale bars, 50 μm.

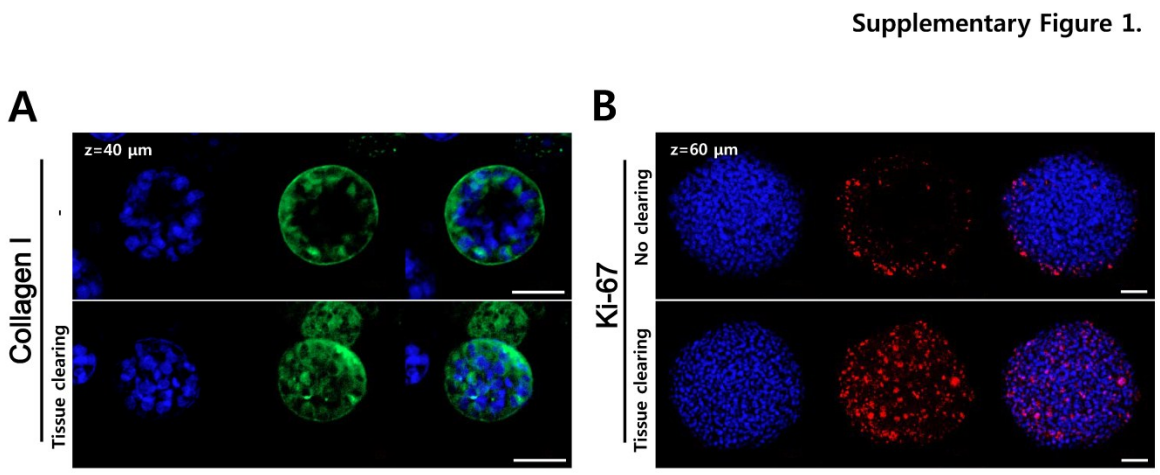

Supplementary video 1. Video showing experimental procedures for high-throughput, high-content histological analysis of 3D tumor spheroids by pillar array. The steps included are; assembly of the pillars in the pillar holder, loading and culturing cancer cells in 3D using 96-

well plates, drug exposure, embedding spheroid arrays in the OCT solution, sectioning the OCT block, and conducting immunohistochemical staining.

Supplementary video 2. A 3D reconstruction image of HT-29 spheroids following exposure to 100 μM of DOX for 20 min. Serial images were obtained by optical sectioning at 9 μm increments over 351 μm distance from the bottom to the center of an alginate cap along the z-axis; images of the region beyond this distance was not acquired due to optical attenuation. Intranuclear accumulation of DOX visualized by fluorescence imaging demonstrated 3D structure of HT-29 spheroids cultured in alginate matrix on pillar array. Approximate sizes of spheroids appeared to be 113 ± 25 μm.